NORSAR Scientific Report No. 2-2007

Semiannual Technical Summary

1 January - 30 June 2007

Frode Ringdal (ed.)

Kjeller, August 2007

6.3 Single small array regional localization using PMCC (ELOSV2)

6.3.1 Introduction - principle of the algorithm and first observations

The Progressive Multi-Channel Correlation Method (PMCC, Cansi, 1995) has been developed at the French Commissariat à l'Energie Atomique (CEA) and is used as a real-time detector for low-amplitude coherent waves within non-coherent noise. It works by performing a progressive association of channels for which the cross-correlation functions are consistent with delay-times (closure time relation) corresponding to coherent seismic energy propagating over an array. The detector is only sensitive to an increased degree of semblance between traces and does not detect directly increases in signal amplitudes.

A new module (ELOSV2) has been developed by CEA for single small-array regional event location using the PMCC results. Phase detection, and the estimation of azimuth and apparent velocity within each time-frequency window, is performed by PMCC. ELOSV2 then applies deterministic criteria to identify seismic phases, and associate them in order to create events.

Firstly, PMCC is run on the recorded data and the time-frequency windows (pixels) are grouped into families under similarity criteria regarding time, frequency, slowness, azimuth, correlation and consistency. The ELOSV2 algorithm then labels the families according to slowness and other criteria, resulting in a seismic phase identification (Pn, Pg, Sn, Lg). Finally, regional events are defined given the detection and association of the appropriate seismic phases. This algorithm has been tested on several months of ARCES data. Fig. 6.3.1 presents a velocity-azimuth histogram of the families detected by ELOSV2 during five months in 2007.

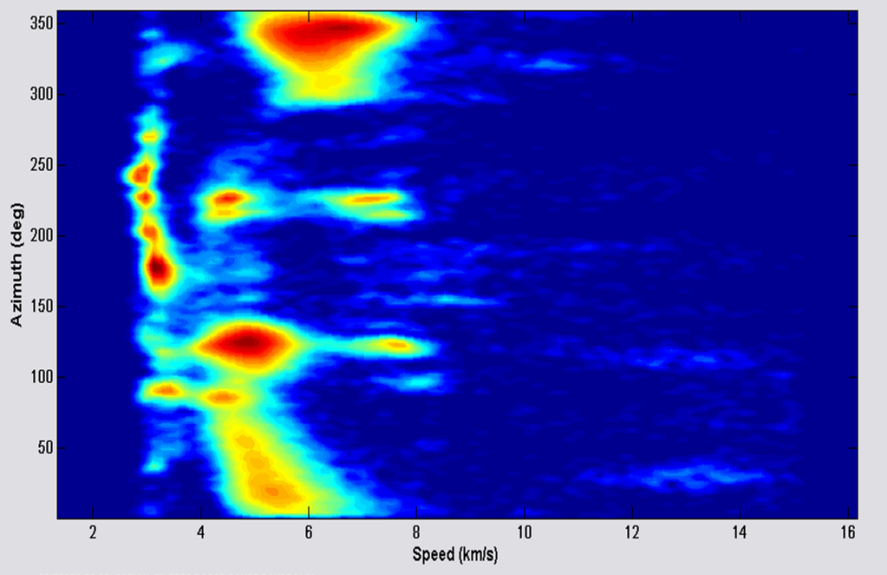

Fig. 6.3.1. Velocity-azimuth histogram of ARCES data between 10 January and 16 May 2007.The data are filtered between 2.5 Hz and 7 Hz, and only the A, B and C rings of ARCES are used for the analysis.

In Fig. 6.3.1, we can identify different kinds of detections. The azimuths around 225˚ and 120˚ are characterized by two distinct groups of energy with different apparent velocities, one around 7.5 km/s and the other around 4.5 km/s. These correspond respectively to P- and S-type regional phases. They cover very distinct azimuth intervals, mostly corresponding to regions of

mining activity. The characteristics of detections from the North (backazimuth around 0˚/360˚) in Fig. 6.3.1 are very different; the detections cover a wide azimuth range and a continuum of apparent velocity estimates that cover the range of regional P- and S- type phases. They are almost always characterized by a low SNR and can be considered to be very coherent high-frequency seismic noise. ELOSV2, in the absence of SNR thresholds, is confronted with long lists of PMCC detections of this nature and creates many regional events from these directions according to fairly arbitrary combinations of such PMCC-phases with typical P- and S-velocities. Far fewer of these event hypotheses appear in the GBF (Ringdal and Kværna, 1989) automatic event bulletin at NORSAR. This is because the GBF associates regional phase detections made using an STA/LTA type detector, and most of the PMCC-detected phases corresponded to SNR below the detection threshold. In the current study, the nature of these observations will be investigated in more detail.

The ELOSV2 algorithm is also applied to data recorded by the Spitsbergen array. SPITS is located to the north of ARCES and may help to locate the source region of seismic energy reaching ARCES from this direction. As a quality check, the output from ELOSV2 is compared with the results of a moving window fk-analysis.

6.3.2 Results

A possible source of very coherent seismic noise coming from the North of Norway had already been observed by Friedrich et al. (1998), who linked low-frequency microseisms observed at different seismic stations in Europe to low-pressure systems in the atmosphere near the northern Norwegian coast. Their observations were made for 1995, DOYs 349, 350 and 351. This time period was also chosen for analysis of ARCES and SPITS data.

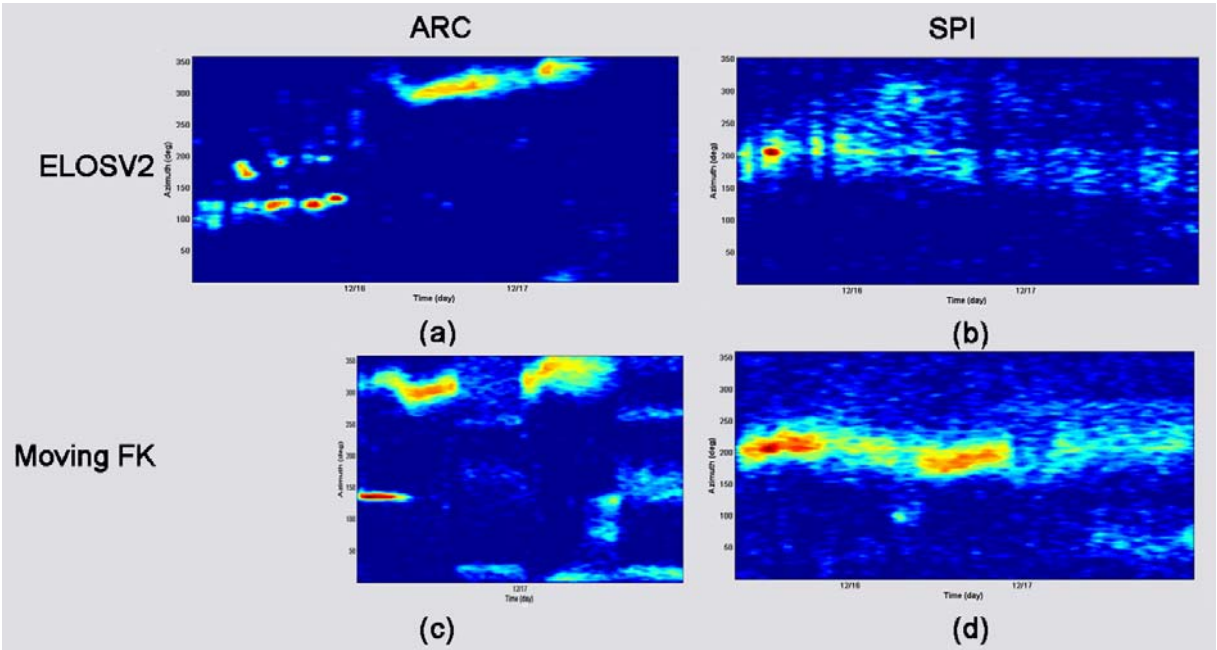

Fig. 6.3.2. Time-azimuth histograms, DOYs 349, 350, and 351 of 1995. (a) ELOSV2, ARCES; (b) ELOSV2, SPITS; (c) Moving fk-analysis, ARCES; (d) Moving fk-analysis, SPITS. The time axes start at about 08 o'clock of DOY 341; due to some data problems, the moving fk-analysis results for ARCES had to be started later (c).

The ELOSV2 processing was performed, together with a moving window fk-analysis, on SPITS and ARCES data from these three days. A "family algorithm" has also been run following the fk-analysis. Fig. 6.3.2 shows the results of this analysis - the time-azimuth histograms obtained for the high frequency (2.5 to 7.0 Hz) calculations of ELOSV2 and moving window fk-analysis.

As we can see in Fig. 6.3.2, the results obtained by the two different methods reveal the same perturbation around the North for ARCES, and from around 200˚ for SPITS. However, the observations begin earlier at SPITS than at ARCES, and the variations of the azimuth are not well correlated.

We have also compared our time-azimuth pattern at ARCES, calculated in the high frequency band 2.5 - 7 Hz, with the pattern at lower frequencies (below 3 Hz). According to Friedrich et al. (1998), this low-frequency energy is related to ocean generated microseisms. It appears that there are significant differences between the high and low frequency time-azimuth patterns, suggesting different source mechanisms.

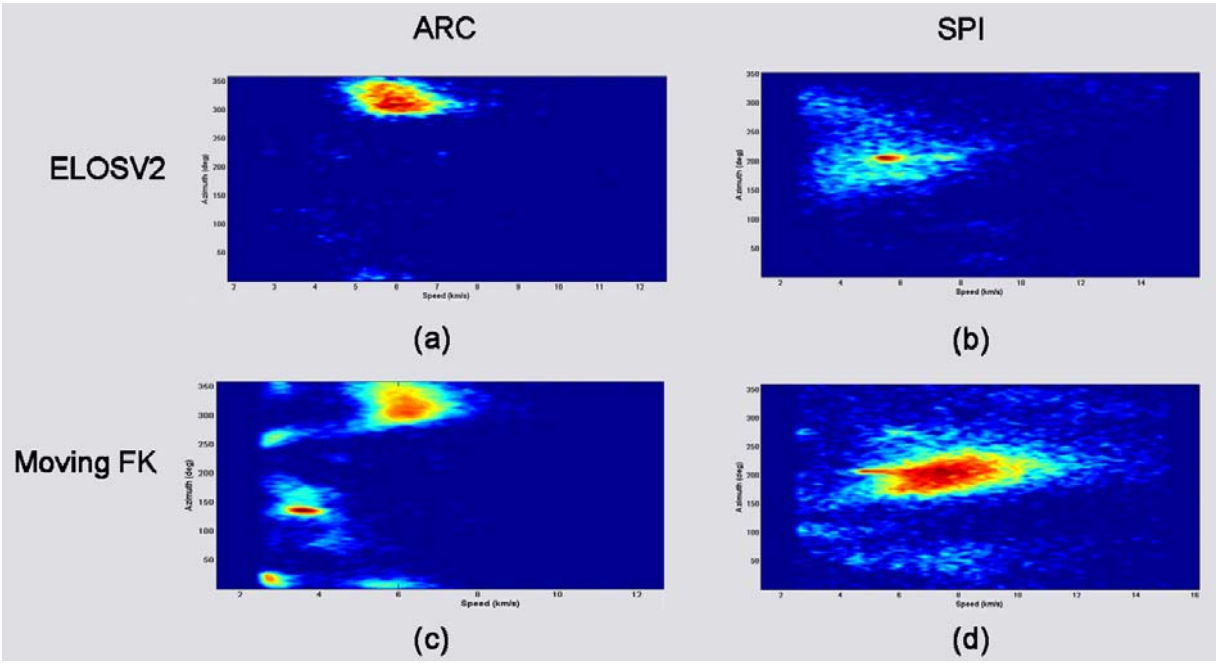

Fig. 6.3.3. Velocity-azimuth histograms, DOYs 349, 350 and 351 of 1995; (a) ELOSV2, ARCES; (b) ELOSV2, SPITS; (c) Moving fk-analysis, ARCES; (d) Moving fk-analysis, SPITS.

The velocity-azimuth histograms are shown in Fig. 6.3.3. Taking into account the frequency range (between 2.5 and 7 Hz) and the velocities measured at the appropriate azimuths (around 6 or 7 km/s), it seems that the observed pulses consist primarily of P-phase type energy.

6.3.3 Discussion

Fig. 6.3.4 shows the evolution (every 6 hours) of three meteorological parameters between DOY 350 at 0 h and 351 at 12 h of 1995, when the higher frequency low amplitude P-wave energy can be observed at ARCES and SPITS. The mean atmospheric air pressure at sea level (on the left, color scale from red/low to blue/high), the mean period of the oceanic waves (in the middle, color scale from green/short to blue/long), and the significant oceanic wave height (on the right, color scale from red/low to blue/high) are displayed.

Fig. 6.3.4 shows a low pressure zone moving between ARCES and SPITS during this period, drawn in red. However, it is difficult to see a direct link with the observations on ARCES or SPITS because the low pressure zone moves too quickly to the East. For example, between DOY 350 at 06 h and DOY 350 at 12 h, the dominant azimuths at ARCES are less than 300˚; while the azimuth of the low pressure zone (in red) is already exceeding 0˚.

At the same time, as seen from Fig. 6.3.4, long periodic oceanic waves with periods of around 8 seconds, and large amplitudes of almost 4 meters height, reach the Norwegian coast over a large range of azimuths. The ocean waves themselves induce the well-documented microseismic noise by interaction with the ocean floor (see, for example, Friedrich et al., 1998). This relatively low frequency noise is linked to the period of the oceanic waves, and propagates with typical surface wave velocities. This is different from what we observe at high frequencies at ARCES and SPITS, where the energy propagation is with typical body wave velocities.

However, it seems that the high frequency P-phase type energy observed at ARCES and SPITS is somehow linked to the presence of these long period, high amplitude ocean waves, even if the azimuths to these proposed source regions do not correspond exactly to the observed azimuths. Open questions are: Why is not more S-type energy observed? How can long periodic ocean waves generate much higher frequency perturbations?

One possible explanation could be that long periodic waves with high amplitudes (i.e. with high kinetic energy) hit the coast as a cascade of single forces. Like a hammer on the free surface, such hits generate compressional waves which propagate in the Earth's crust. The frequency content of these compressional waves can be much higher than the original period of the oceanic waves. This period is then defining the time interval between two successive hits.

To test this hypothesis, the signal pulses observed by the moving window fk-analysis were investigated. Fig. 6.3.5 shows a histogram of the time interval between two successive pulses observed on day 350 at SPITS (see Fig. 6.3.2, d). It is obvious that there is a dominance of time intervals between 4 and 10 seconds. This corresponds quite well with our hypothesis. However, further investigations are needed to come to consolidate this explanation. The peak for 20 seconds is an artefact of the algorithm that calculates the onset families.

Time	Mean Pressure at Sea Level	Mean Wave Period	Significant Wave Height
0 h	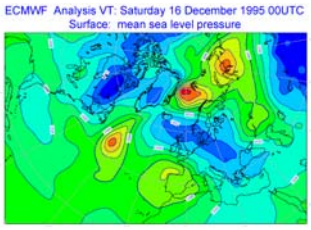	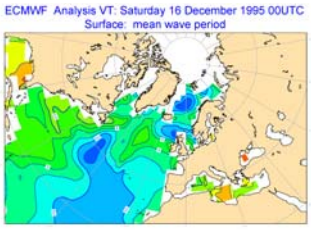	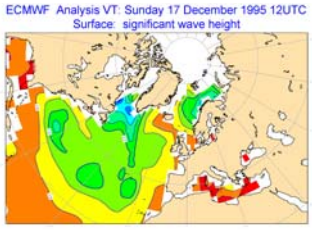
6 h	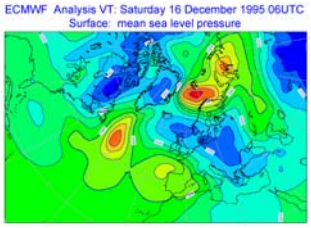	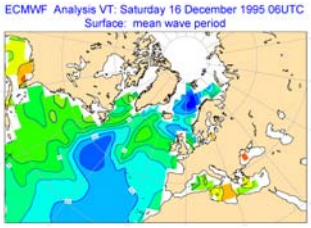	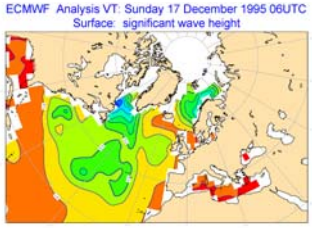
12 h	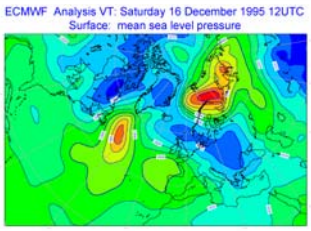	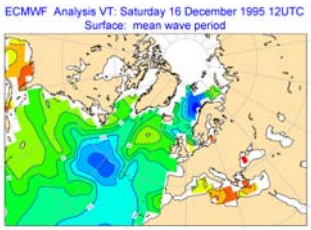	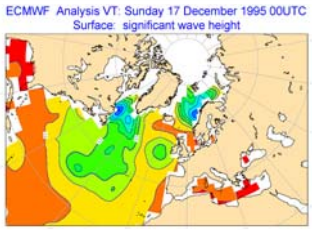
18 h	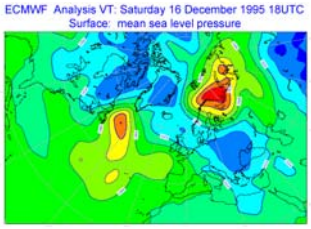	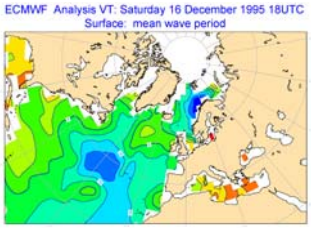	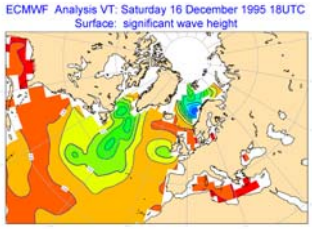
0 h	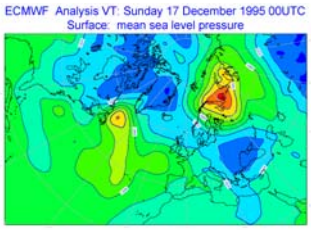	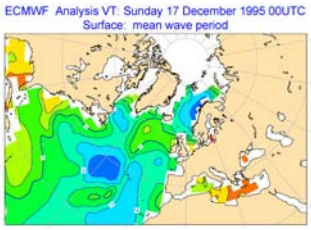	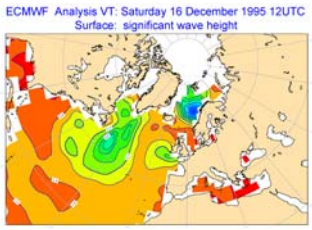
6 h	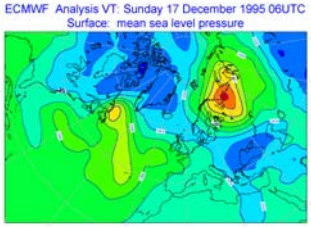	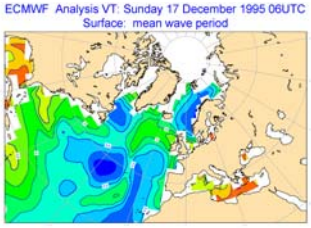	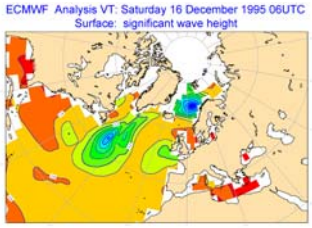
12 h	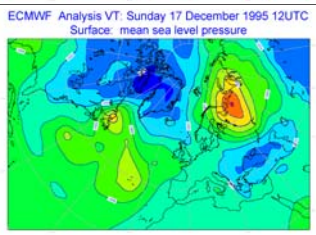	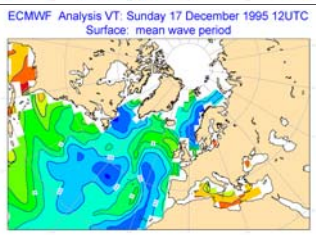	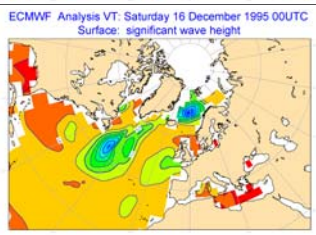

Fig. 6.3.4. Meteorological data for DOYs 350 and 351 in 1995 in the North Atlantic and Barents Sea Region (from the ECMWF data server*); for more details see text.*

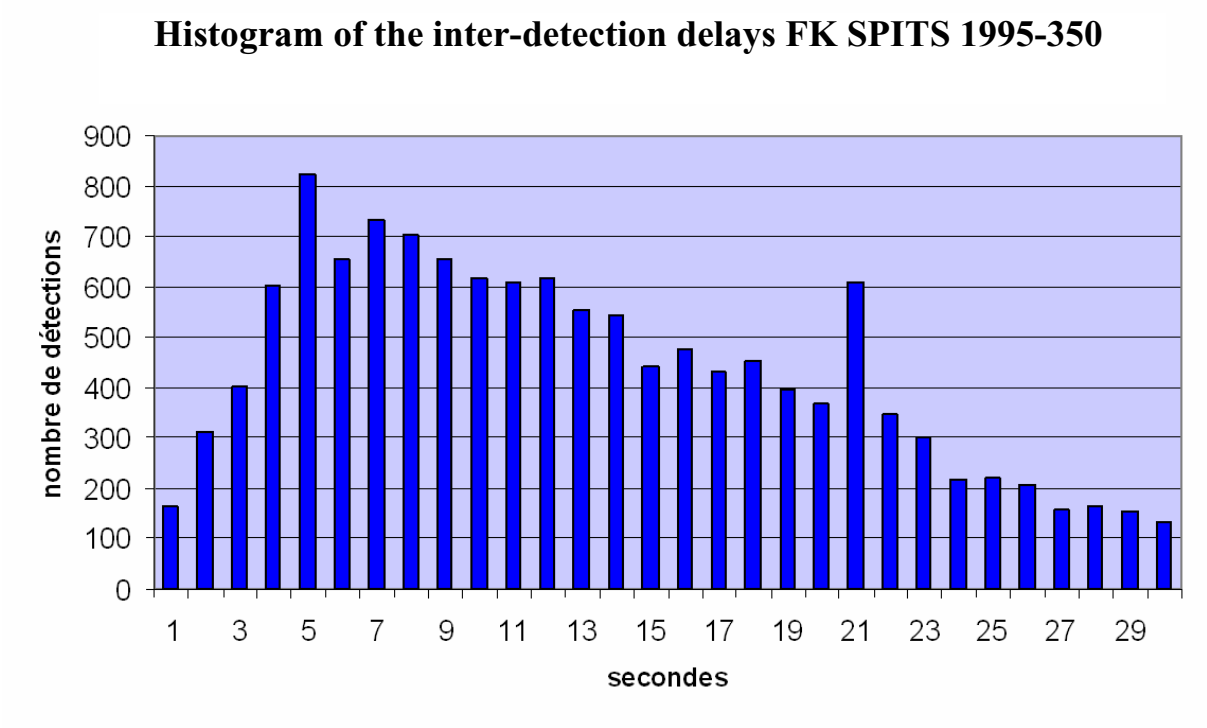

Fig. 6.3.5. Histogram of the time interval between two successive signal pulses applying the moving window fk-analysis for SPITS data on DOY 350 in 1995.

Acknowledgements

Juliette Chabassier's research visit at NORSAR had been made possible under the Transnational Access part of the EC-Project NERIES (EC-Contract No. 026130).

The ECMWF (European Centre for Medium-Range Weather Forecasts) ERA-40 data (Uppala et al., 2005) used in this study have been obtained from the ECMWF data server (http:// data.ecmwf.int/data/d/era40_daily/).

Juliette Chabassier, CEA
Johannes Schweitzer

References

Cansi, Y. (1995). "An automatic seismic event processing for detection and location: The P.M.C.C. method." *Geophys. Res. Lett.*, **22**, pp. 1021-1024.

Friedrich, A., Krüger, F., and Klinge, K. (1998). "Ocean-generated microseismic noise located with the Gräfenberg array." *Journal of Seismology*, **2**, pp. 47-64.

Ringdal, F., and Kværna, T. (1989). "A multi-channel processing approach to real time network detection, phase association, and threshold monitoring. *Bull. Seism. Soc. Am.*, **79**, pp. 1927-1940.

Uppala, S.M., Kållberg, P.W., Simmons, A.J., Andrae, U., da Costa Bechtold, V., Fiorino, M., Gibson, J.K., Haseler, J., Hernandez, A., Kelly, G.A., Li, X., Onogi, K., Saarinen, S., Sokka, N., Allan, R.P., Andersson, E., Arpe, K., Balmaseda, M.A., Beljaars, A.C.M., van de Berg, L., Bidlot, J., Bormann, N., Caires, S., Chevallier, F., Dethof, A., Dragosavac, M., Fisher, M., Fuentes, M., Hagemann, S., Hólm, E., Hoskins, B.J., Isaksen, L., Janssen, P.A.E.M., Jenne, R., McNally, A.P., Mahfouf, J.-F., Morcrette, J.-J., Rayner, N.A., Saunders, R.W., Simon, P., Sterl, A., Trenberth, K.E., Untch, A., Vasiljevic, D., Viterbo, P., and Woollen, J. (2005): The ERA-40 re-analysis. Quart. J. R. Meteorol. Soc., **131**, 2961-3012, doi:10.1256/qj.04.176.